INSTITUT foton

Highlights 2018

UNIVERSITÉ DE RENNES 1

cnrs

INSA INSTITUT NATIONAL DES SCIENCES APPLIQUÉES RENNES

SPM Physique Chimie Mécanique

iut Lannion

IMT Atlantique Bretagne-Pays de la Loire École Mines-Télécom

ENSSAT LANNION

FOREWORD

This document is a digest of **scientific highlights selected** among the results obtained during year **2018** by the teams and platforms(*) of Institut FOTON (CNRS UMR 6082). By browsing these pages the reader will get a flavor of the on-going research topics in our laboratory, that are organized around <u>six axes</u>:

Axis I: Devices and functionalities for optical communications

Axis II: Microwave, millimeter-wave, and THz optics

Axis III: Innovative materials for photonics

Axis IV: Instrumentation, optical sensors and coherent imaging

Axis V: Advanced concepts for photovoltaics

Axis VI: Physics and metrology of lasers

Each highlight corresponds to an article published in an international peer-reviewed journal. The reader will find **additional information through that reference**, or by **contacting** the mentioned **laboratory member**.

Please visit also the laboratory **website** : http://foton.cnrs.fr/

(*)The Institut FOTON is composed of <u>three research teams</u>:

- ***DOP*** *team (Univ. Rennes 1 / CNRS), Rennes Beaulieu – Head: F. Bondu*
- ***OHM*** *team (INSA / CNRS), Rennes INSA - Head: C. Cornet*
- ***SP*** *team (Univ. Rennes 1 / CNRS), Lannion ENSSA – Head: M. Thual*

and <u>three platforms:</u>

- ***CCLO*** *(Univ. Rennes 1 / CNRS), Lannion ENSSAT – Head: M. Guendouz*
- ***PERSYST*** *(Univ. Rennes 1 / CNRS), Lannion ENSSAT – Head: C. Peucheret*
- ***NANORENNES*** *(INSA / Univ. Rennes 1 / CNRS), Rennes INSA – Head: C. Paranthoën*

CONTENTS

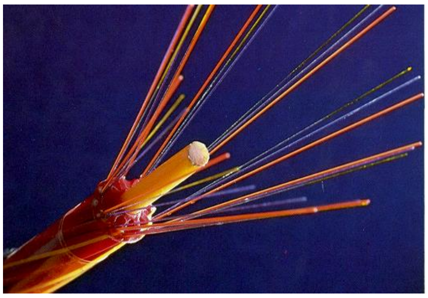

IMAGING THE WHISPERING GALLERY MODES OF A MICRODISK RESONATOR

OHM / SP

Hyperspectral cathodoluminescence is used to image at a sub-microscale resolution tens of whispering gallery modes simultaneously in an active semiconductor microdisk resonator as shown in Figure a (Scanning electron microscopy).

Whispering gallery mode (WGM) resonators are essential building blocks of on-chip photonics. However, the geometrical features of these objects usually prevent people from direct observation of WGMs, limiting their characterization to the sole spectral information.

In this work, the high spatial and spectral resolutions (100nm and 0.1nm respectively) of hyper spectral cathodoluminescence is used locally probe the local density of optical states (LDOS) in a GaP microdisk through the emission of GaPN quantum wells (see figure b). At low temperature (5K), these emitters offer all the required features for such an experiment: a high quantum efficiency, strong carrier localization ensuring high spatial resolution, the spatial homogeneity of the emitter properties and finally a broad emission spectral range.

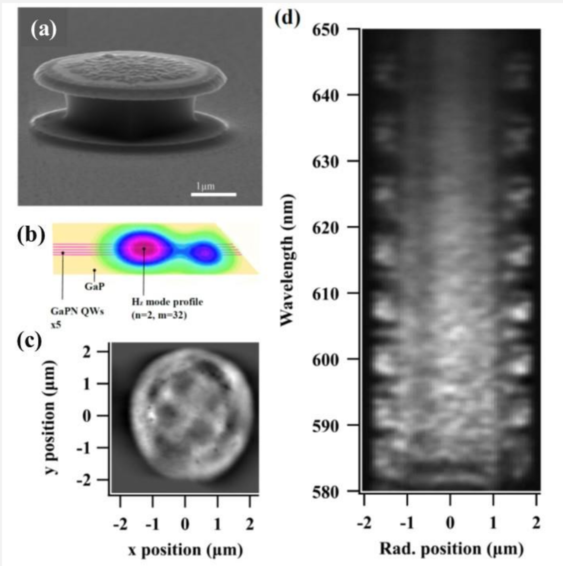

For each (x,y) position of the scanning electron beam, the emission spectrum of the GaPN quantum wells, filtered by the microdisk optical modes, is collected. Advanced Fourier filtering is then used on the resulting 4D dataset to keep track of the WGMs signal only. At fixed wavelength, each WGM can thus be imaged spatially (see Figure c, 584.5nm mode) while the LDOS can also be analyzed in a spectral-radial plane (see Figure d).

This LDOS mapping was then compared to finite element simulations of optical modes in microdisks of different geometries. We discovered that the microdisk LDOS contains sufficient information to extract both the radial order of WGMs and their polarization state (TE/TM). The spectral ordering of these different mode families is strongly influenced by the resonator geometry such as a wedge along the microdisk rim for example.

Our results show the relevance of hyperspectral cathodoluminescence as an ultimate characterization tool for advanced photonic engineering.

Contact

yoan.leger@insa-rennes.fr

Reference

“Cathodoluminescence hyperspectral analysis of whispering gallery modes in active semiconductor wedge resonators”, P.Guillemé *et al.*, *Opt. Lett.* **43** 1766-1769 (apr 2018)

hal-01770934

« The LDOS contains sufficient information to extract both the radial order and polarization state of WGMs »

More Information

- hal.archives-ouvertes.fr/hal-01529567
- hal.archives-ouvertes.fr/hal-01396654

Collaborations

- Attolight SA (Switzerland)
- Institut de recherche mathématique de Rennes (France)

attolight IRMAR

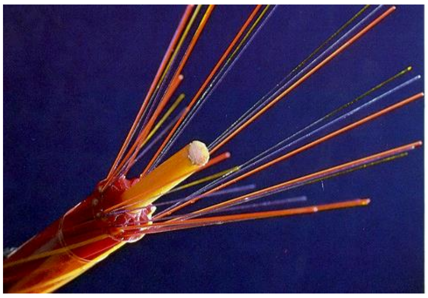

GENERATION OF SINGLE-SIDEBAND PAM4 SIGNALS

SP

Contact

laurent.bramerie@enssat.fr

Reference

“Dispersion uncompensated Transmission of NRZ and PAM-4 Single-Sideband Signals using D-EML”, M.E.Chaibi, L.Bramerie1, D.Erasme, C.Peucheret, *Optical Fiber Communication Conference (OFC 2018), San Diego, United States. Tu2.C3 (mar 2018)*

hal-01754007

Single-sideband (SSB) optical signals are well known for their improved spectral efficiency and their better tolerance to chromatic dispersion effects compared to double-sideband (DSB) signals in intensity-modulation (IM) and direct detection (DD) transmission links. Optical SSB signals can be generated using either in-phase and quadrature (I/Q) modulators or optical filters. The first alternative requires bulky and relatively expensive modulators while the use of optical filtering to generate vestigial-sideband signals induces tight alignment tolerance, making both schemes unsuitable for access and interdata-center networks. The dual-modulation technique, combining a directly-modulated distributed-feedback (DFB) laser and an electroabsorption modulator (EAM) has been proposed to generate optical SSB signals with sufficient bandwidth in a cost-effective and energy-efficient way. In this technique, the DFB realizes frequency modulation (FM) through its frequency chirp and the EAM performs intensity modulation (IM). Optical SSB signals can thus be generated following the synthesis of a suitable frequency-modulating signal applied to the DFB. The feasibility of this technique has been so-far only demonstrated with analog-waveform modulation formats, including orthogonal frequency division multiplexing (OFDM) and carrier-less amplitude and phase (CAP) signals.

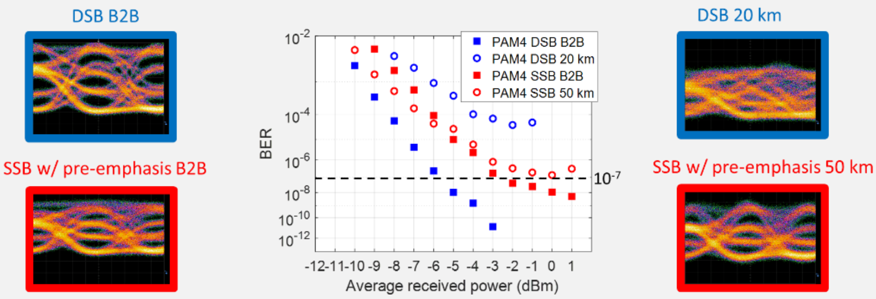

In this paper, we demonstrate for the first time to our knowledge the generation of optical SSB PAM-4 signal at 10.7 Gbps using a monolithically-integrated D-EML. This is made possible thanks to the application of a proper pre-emphasis to the signal driving the EAM in order to compensate residual intensity ripples generated in the DFB section. Dispersion uncompensated transmission of the signal is achieved with error-free performance over 50-km standard single-mode fiber (SSMF), which is not possible with a DSB signal generated with the same laser. The enhancement brought by the pre-emphasis on the EAM driving signal is also assessed. The SSB modulation suffers from 7-dB power penalty at 10^{-9} BER in back-to-back, and the introduction of the proposed pre-emphasis scheme reduces this penalty to 4 dB.

« To mitigate the unwanted IM modulation generated in the DFB laser section, an effective pre-emphasis scheme applied to the EAM driving signals has been proposed »

Collaborations

- Telecom ParisTech (France)

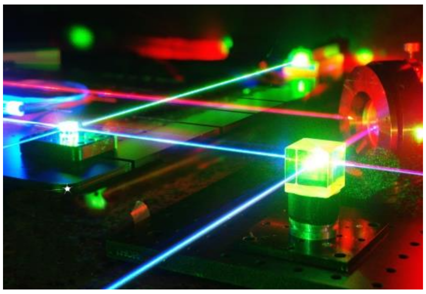

HIGHLIGHTS

ULTRASTABLE MICROWAVE-OPTICAL EMISSION FROM DFB FIBER LASERS

DOP

Contact

marc.brunel@univ-rennes1.fr

Reference

"Beat note stabilization in dual-polarization DFB fiber lasers by an optical phase-locked loop", M. Guionie *et al.*, *Opt. Express* **26** 3483-3488 (2018)

hal-01716235

« Ultra-narrow carrier at 1GHz stays locked for days, and the scheme is scalable »

More Information

- doi.org/10.1038/nphoton.2007.89
- doi.org/10.1109/JLT.2008.2009551

Collaborations

- iXblue Photonics (France)

Fiber lasers are appealing sources for a wide variety of applications because of their compactness, ruggedness, and ease of integration. Distributed-feedback (DFB) fiber lasers in particular, that are usually designed to be single frequency, show remarkable performances (low noise, narrow line-width) as compared to their semiconductor counterparts. In the field of microwave photonics, dual-frequency lasers of various kinds have found great interest for the generation and distribution of tunable high-purity signal carriers from the GHz to the THz ranges. It has long been shown that these DFB fiber lasers are capable of sustaining the oscillation of two orthogonal polarizations at different frequencies, but stabilization of the beat note had never been realized in DFB fiber lasers. Why stabilization? In the context of optical distribution of local oscillators in radio-over fiber for instance, stabilization of the beat frequency is mandatory, because the frequency reference has to be distributed to different stations, and the natural drift of the laser beat is a limitation.

In this work, we have studied a fully fibered microwave-optical source at 1.5 µm. It is shown that the beat note between two orthogonally polarized modes of a DFB fiber laser can be efficiently stabilized using an optical phase-locked loop (OPLL where the pump-power-induced birefringence can serve as an actuator of the laser beat note. Working with different samples provided by our partner iXblue Photonics in Lannion, beat notes at 1 GHz and 10 GHz were successfully stabilized to a reference synthesizer, passing from the 3 kHz free-running linewidth to a stabilized sub-Hz linewidth, with a phase noise as low as –75 dBc/Hz at 100 Hz offset from the carrier.

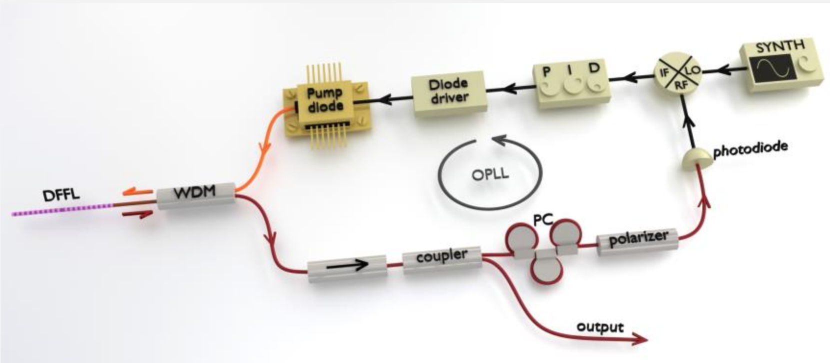

Such dual-frequency stabilized lasers offer compact integrated components for RF and microwave photonics applications. Subsequent work shows that other stabilization schemes, such as frequency-shifted optical feedback, are possible. Finally, other short fiber laser structures, namely DBRs, are also under investigation, and could meet another expected feature of microwave optical sources: tuning to higher frequency carriers, like the 3.5 GHz or 26 GHz frequency bands for 5G communication systems and beyond.

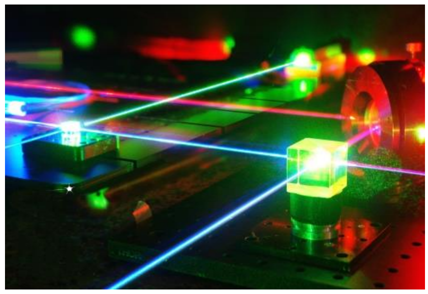

COUPLED MICRORESONATORS FOR MICROWAVE GENERATION

SP

Contact

yannick.dumeige@univ-rennes1.fr

Reference

“Microwave generation on an optical carrier in microresonator chains”, A.Armaroli *et al.*, *Phys. Rev. A* **98** 013848 (jul 2018)

hal-01939635

We consider self-pulsing regimes in chains of Kerr nonlinear optical microresonators. By means of a supermodal diagonalization procedure of the conventional coupled-mode theory in time, we theoretically and numerically study the bifurcation diagrams of a singly pumped three-cavity and a doubly pumped four-cavity system: the latter allows us to predict thresholdless frequency tripling of a GHz modulation. These self-pulsing regimes are proven robust and will find applications in the generation and conversion of microwaves on an optical carrier.

Based on a diagonalization procedure of the coupled-mode theory in time, which allows us to write the nonlinear equations which rule the coupling between supermodes in a chain of Kerr-nonlinear optical microresonators, we present a thorough bifurcation analysis of (i) degenerate four-wave mixing in a three-cavity chain, and (ii) nondegenerate four-wave mixing in a four-cavity chain. Their bifurcation diagrams and behavior in phase space are similar in many aspects (multistability of limit cycles, NS bifurcations, phase locking between injection and pump and between pump and sidebands). The main difference relies on the thresholdless microwave generation in the four-cavity system. A sensible set of parameters is presented to show the accessibility of these oscillatory regimes. Moreover, the exploration of the parameter space by means of Monte Carlo simulations allows us to estimate the robustness of the present solutions to technological inaccuracies. The result indicates that the four-cavity solution is less robust (tolerating quite a smaller uncertainty level), but still achievable in current technological platform.

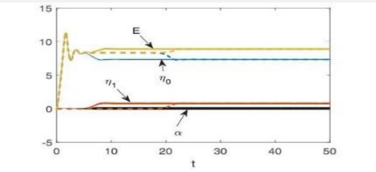

FIG. 2. Comparison of the evolution toward the steady state of the three-cavity system and its three-mode truncation. $P = 40$, $\delta = -3$, $\gamma = 40$. Solid lines represent the solution of Eq. (2), while dashed lines represent the solution of Eq. (5): η_0 is in blue (dark-gray upper line), η_1 in red (gray at the bottom), E in yellow (light gray at the top), and the imbalance α is in black (at the bottom) [only for Eq. (2)]. Notice that the last one exhibits small oscillations around zero. The other quantities reach the steady state more slowly in Eq. (5) than in the original model, but represent quite an accurate approximation of the system behavior.

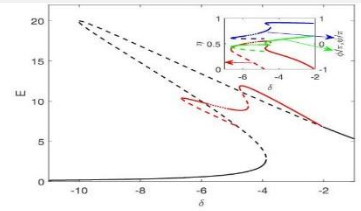

FIG. 3. Bifurcation diagram with $P = 40$. The main panel shows the bistable curve of E as a function of δ (bifurcation parameter) of fixed points of Eq. (5), with $\eta = 1$, in black, and limit cycles, $\eta \neq 0, 1$, in red (gray). Solid lines represent stable limit cycles, dashed lines represent unstable ones (saddle points), and dotted lines are delimited by Neimark-Sacker bifurcations. The inset shows the bifurcation of the other three variables: η [red (gray), left axis], ϕ_1 [green (light gray), right axis], and ψ [blue (dark gray), right axis].

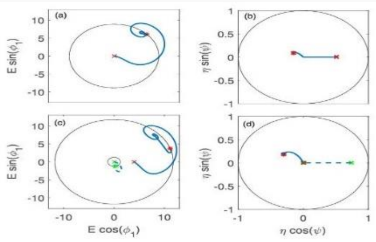

FIG. 4. Phase-space representations of the time evolution of Eq. (5). (a), (c) The plane ($E \cos \phi_1$, $E \sin \phi_1$), with the circles denoting steady E's. (b), (d) The plane ($\eta \cos \psi$, $\eta \sin \psi$), with the unit circles included for reference. (a), (b) Correspond to Fig. 2. Cold-cavity (random noise in each mode) initial conditions (red crosses) are used, where the blue line represents the evolution and the red asterisk represents the attained steady state. (c), (d) The solutions for $\delta = -4.5$, at fixed $P = 40$, for two different initial conditions: cold and hot cavity. The former [dashed line, with green (light gray) markers] collapses rapidly to the lower branch fixed point, while the latter (solid line) is attracted to an oscillating solution.

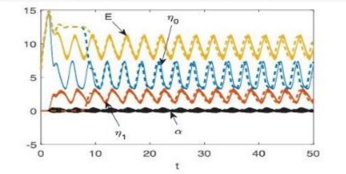

FIG. 5. Same as Fig. 2, but with $\delta = -5.5$ and hot-cavity initial conditions $u_0 = 2.5$ and $u_{\pm 1} = 0$. The limit cycles here are unstable and the system oscillates on a torus; the secondary frequency is much smaller the main one. The average conversion to sidebands is about 25%.

« We prove that in the large coupling coefficient regime, a microwave frequency Ω can be converted with high efficiency to 3 Ω with up to 50% of the total energy inside stored in the cavity system »

Collaborations

- Université de Genève (Switzerland)

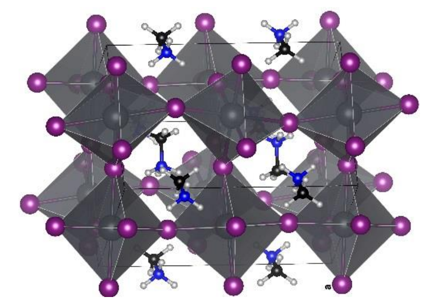

Contact

charles.cornet@insa-rennes.fr

Reference

"Universal description of III-V/Si epitaxial growth processes", I. Lucci *et al.*, *Phys. Rev. Mater.* **2** 060401(R) (jun 2018)

hal-01833206

« Most of the structural III-V/Si defects fundamentally originate from the partial wetting of III-V semiconductors on silicon »

More Information

- hal.archives-ouvertes.fr/hal-01803990
- doi.org/10.1063/1.5055056

Collaborations

- Institut de Physique de Rennes (France)
- Centre d' Élaboration de Matériaux et d'Études Structurales (France)
- Institut d'Elctronique et des Systèmes (France)
- Centre de recherche sur l'hétéroepitaxie et ses applications (France)
- Centre de Nanosciences et de Nanotechnologies (France)

UNIVERSAL DESCRIPTION OF III-V/SI EPITAXIAL PROCESSES

OHM

The monolithic integration of III-V semiconductors on the low cost silicon substrate is a main concern in today's materials research. Indeed, the successful combination of III-V and Si semiconductors opens many routes toward integrated photonic devices, and energy applications, such as photovoltaics or solar hydrogen production from water. Materials researchers however face the issue of crystal defects appearing at the III-V/Si interface during the materials growth, and especially the creation of the so-called antiphase domains (APDs). Without a clear picture on the origin of defects generation, scientists have developed some strategies using thick buffer layers to bury these defects that are detrimental for photonic and photovoltaic applications.

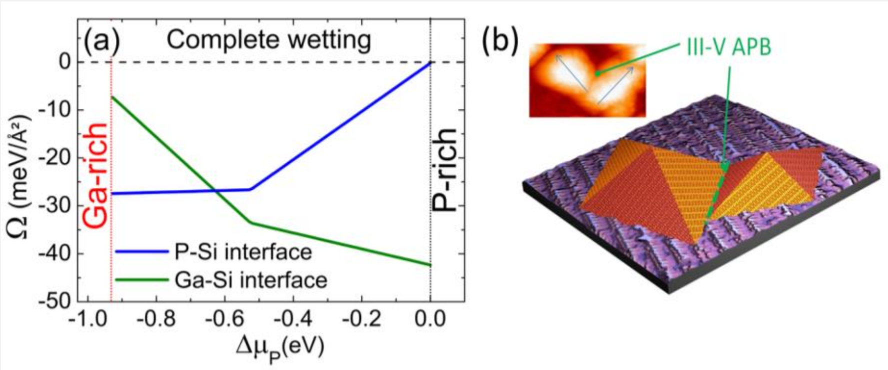

Here, we clarify III-V/Si crystal growth processes. Microscopy shows that monodomain 3D islands are observed at the early stages of AlSb, AlN, and GaP epitaxy on Si, independently of misfit. It is also shown that complete III-V/Si wetting cannot be achieved in most III-V/Si systems, by calculating the spreading parameter from surface and interface energies determined by the density functional theory over the full range of chemical potentials (Fig. (a)). Surface/interface contributions to the free-energy variations are found to be prominent over strain relief processes. We finally propose a unified description of III-V/Si growth processes, including a description of the formation of antiphase boundaries (Fig. (b)). Generation of APDs in III-V/Si epilayers is thus governed by the respective area ratio of the different Si terraces orientations, and not to the monoatomic steps areal density as usually suggested. Overall, we finally conclude that most of the structural defects usually formed during III-V/Si epitaxy (twist, tilt, imperfect dislocations networks or APDs) fundamentally originate from the partial wetting of III-V semiconductors on silicon, without a significant impact of elasticity. This generalized description of III-V/Si growth processes opens new routes to deeply co-integrate photonics and electronics.

MID-IR PHOTOLUMINESCENCE FROM Pr^{3+}-DOPED CHALCOGENIDE

SP

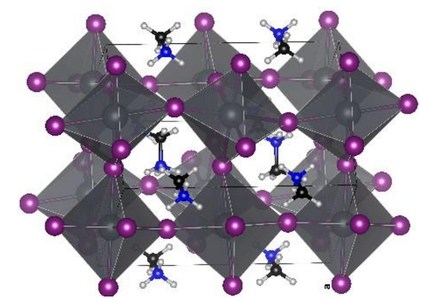

There is a growing interest for broadband light sources and amplifiers operating in the mid-infrared (mid-IR) and especially in the 3-5 µm spectral window for sensing applications (Figure a)). Rare earth (RE)-doped chalcogenides glasses are promising candidates to implement integrated mid-IR lasers and amplifiers.

Praseodymium-doped selenide thin films are deposited by radio frequency magnetron sputtering on thermally oxidized silicon wafers and undoped selenide layers. Ridge waveguides are then processed using photolithography and dry etching techniques (Figure c)). Under optical pumping at 1.55 µm, broadband guided mid-infrared photoluminescence is recorded for the first time for wavelengths above 4 µm from rare earth-doped integrated chalcogenides waveguides. Photoluminescence was recorded for various waveguides dimensions and for various pumping power and in particular for ridge waveguide allowing single-mode optical propagation at 2.5 µm and 4.70 µm (Figures d) and e)). These results confirm the potential of RE-doped chalcogenides for the development of low-cost on-chip mid-IR amplifiers or lasers.

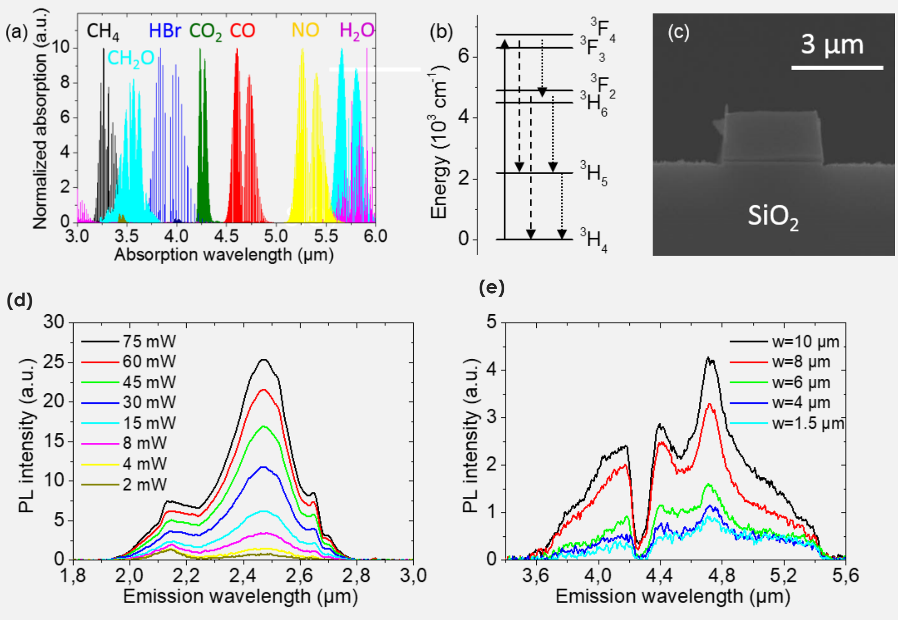

a) Absorption bands of selected molecular species in the mid-IR range
b) Simplified low energy part of the energy level diagram of Pr^{3+} ions
c) Scanning electron microscope image of the processed waveguide after ICP-RIE,
Mid-IR PL (λ_{exc}=1550 nm) spectra recorded
d) for different optical excitation densities
e) and for different Pr^{3+}-doped selenide ridge waveguide widths.

Contact

loic.bodiou@univ-rennes1.fr
joel.charrier@univ-rennes1.fr

Reference

"Mid-infrared guided photoluminescence from integrated Pr3+-doped selenide ridge waveguides", L.Bodiou *et al.*, *Opt. Mater.* **75** 09-115 (jan 2018)

hal-01639691

« First demonstration of mid-IR guided photoluminescence from rare earth-doped integrated chalcogenides waveguides»

Collaborations

- Institut des Sciences Chimiques de Rennes (France)
- Centre de recherche sur les Ions, les MAtériaux et la Photonique (France)
- University of Pardubice (Czech Republic)
- Politecnico di Bari (Italy)

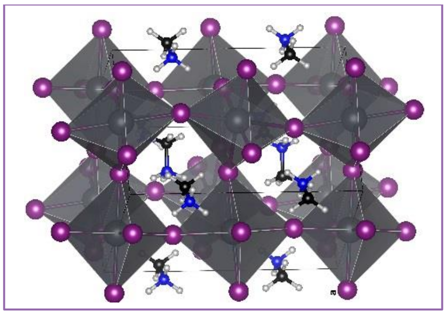

Contact

nathalie.lorrain@univ-rennes1.fr
mohammed.guendouz@univ-rennes1.fr
joel.charrier@univ-rennes1.fr

Reference

"Multilayer structures based on porous silicon for photonic applications in the Mid Infra-Red", P.Girault *et al., 11th Porous Semiconductors - Science and Technology 2018 Conference* (mar 2018)

hal-01891935

« First fabrication of multilayer structures based on Porous silicon for Mid-IR sensing applications »

Collaborations

- Institut d'Électronique de Microélectronique et de Nanotechnologie (France)
- Lumière, Nanomatériaux, Nanotechnologies (France)

HIGHLIGHTS

POROUS SILICON VERTICAL MULTILAYER STRUCTURES FOR MID-IR

SP

The ability to tailor Porous Silicon (PSi) refractive index and layer thickness by controlling porosity and anodization time makes it especially attractive for optical applications. Moreover, PSi is also biocompatible material and its functionalization by grafting molecules to detect is interesting for surfacic detection due to its high specific surface up to 800 m^2/cm^3.

The implementation of a Mid Infra-Red (Mid-IR) silicon photonics transducer by using vertical multilayer structures based on Si with broad Mid-IR transparency (up to 8 µm) is a challenge that could find applications in spectroscopic sensing and environmental monitoring.

From the refractive index and the growth rate knowledge of the PSi layers, the design of vertical multilayers structures is performed in order to determine the best combination of parameters of Bragg reflectors and cavities: reflection bandwidth Δλ, resonance wavelength and maximum reflectance. Some examples of micrographs of prepared multilayered structures obtained by scanning electron microscope (SEM) are presented in figure 1 (a, b). The interfaces between individual layers as well as the surfaces of the multilayered structures were found to be smooth without any defect during the fabrication of thin film stacks.

The experimental reflectivity spectra are shown in Figure 1 (c, d) respectively for Bragg reflector and micro-cavities centered at 6500 nm. This work demonstrates that it is possible to produce vertical multilayer structures with good optical qualities in the Mid-IR range from PSi layers.

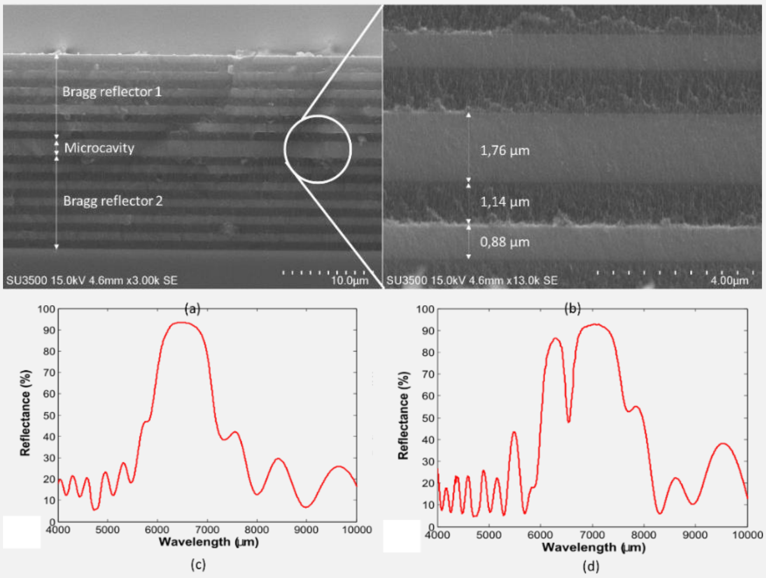

Figure 1: SEM micrographs of vertical multilayer structures (a) and (b). Experimental reflectivity spectra of (c) PSi Bragg reflector and (d) PSi vertical micro-cavity, centered at 6500 nm.

Polarizer-free polarization contrast compressive imaging

DOP

Compressive sensing approaches for signal acquisition/reconstruction and imaging have raised a strong interest these last years on many applications. In the context of polarimetric imaging, where complexity, time-consumption and difficulty of interpretation still hinder the spreading of such imaging techniques in applications, compressive sensing appears as a promising trail to develop simplified and robust polarimetric imaging systems at wavelengths were imaging sensors or polarimetric optical components are not available. This trail is remained so far very little explored, and the existing contributions have limited themselves to simplistic detection scheme consisting of adding a polarimetric analyzing element (more or less complex) to a standard compressive imaging setup.

To revisit the approach of compressive sensing-based polarimetric imaging, we have recently proposed an original concept of compressive acquisitions for polarimetric contrast imaging, relying on the use of a digital micromirrors device (DMD), and two single-pixel detectors, but without any polarization analyzing element. The polarimetric sensitivity of the imaging scheme proposed relies on the diversity of the Fresnel's reflection coefficients of the reflective mirrors, which vary slightly for different incidence angles and for distinct polarization components. This property is exploited in this setup to form an original reconstruction problem, which combines a compressed sensing recovery problem with a source separation task. We have numerically demonstrated the capacity of such a system to produce polarimetric contrast images after reconstruction from simulated temporal signals on the two photodiodes

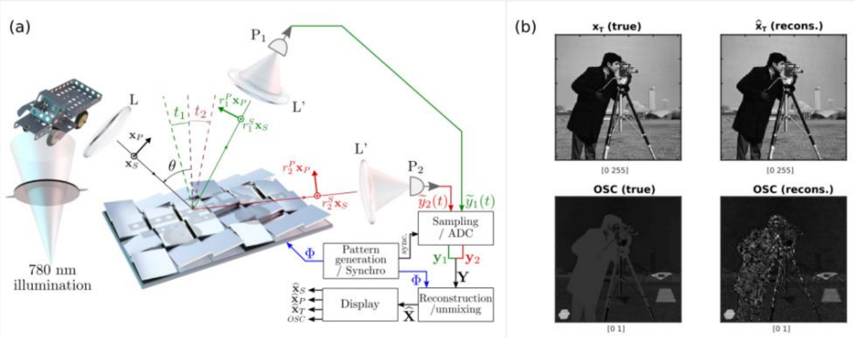

For that purpose, we have proposed a dedicated joint recovery method (implemented through a reweighted FISTA algorithm), which outperforms a more simplistic two-step approach (reconstruction, then inversion of the mixing matrix of the polarimetric components). Further improvement in reconstruction quality can be obtained at low signal-to-noise ratio by including physical constraints, specific to the context of polarimetric imaging, in the recovery process (which is implemented through an iterative Generalized Forward-Backward (GFB) algorithm). It must be noted here that the proposed architecture does not require either polarimetric analyzing element, or array detector, thus paving way for the design of polarization-sensitive imaging systems in spectral ranges were usual techniques fail.

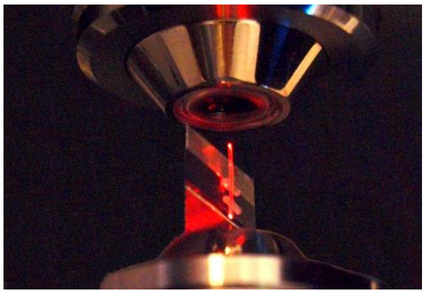

Contacts

julien.fade@univ-rennes1.fr

Reference

"Polarizer-free two-pixel polarimetric camera by compressive sensing", J. Fade *et al.*, *Appl. Optics* **57** B102-B113 (mar 2018)

hal-01673537

« Reconstructing polarization contrast compressive imaging from two single-pixel detectors... »

More Information

- Funded by Univ. of Rennes 1 & European Research Council (J. Bobin)

Collaborations

- Institut de Recherche sur les lois Fondamentales de l'Univers (France)

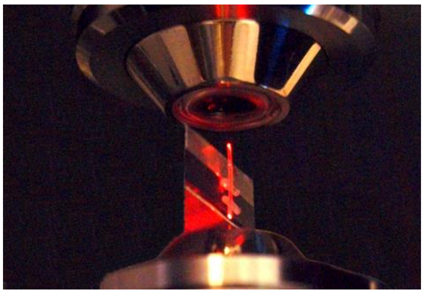

HIGHLIGHTS

LIQUID CRYSTAL BASED TUNABLE PHOTODIODES OPERATING AT 1.55 µM

OHM

Contact

christophe.levallois@insa-rennes.fr

Reference

"Liquid crystal-based tunable photodetector operating in the telecom C-band", C. Levallois *et al.*, *Opt. Express* **26** 25952-25961 (oct 2018)

hal-01879162

« The demonstration of this tunable photodiode as a micro-spectrometer has been also achieved »

Miniaturized tunable photodetector (Tun-PD) can be of great interest for applications wavelength division multiplexing systems. For these optical communications systems, point-to-point transmission links require the use of dynamically-reconfigurable 1.55 µm devices. This type of PD can also find an interest in the development of compact and reconfigurable optical sensor, or the realization of micro-spectrometer. Previous works on Tun-PD or micro-spectrometers are mainly based on the modulation of the physical length of a microcavity thanks to the actuation of a movable mirror. A promising alternative to this MEMS-based approach consists in the integration of a liquid crystal (LC) layer inside a microcavity monolithically integrated on a PD. Recently, we report for the first time InGaAs based PD integrating LC microcells resonant microcavity on their surfaces, acting as a wavelength selective filter part of the integrated device. Fig. (a) illustrates the sample at the end of the fabrication process where each LC microcell contains an array of 9 PDs, when fig. (b) gives a 3D view of a single Tun-PD. The physical principle of wavelength selection relies on the modulation of the refractive index of the thick LC layer (6 µm) surrounded by two Bragg mirrors. As indicated in fig. (c), when no driving voltage is applied on the LC microcell, the LC are parallel to the surface of the sample, and the refractive index is then maximum. When this voltage is increased, the LC molecules are reoriented leading to a decrease in the refractive index for the light polarized along the initial orientation of the LC molecules. Therefore, resonant wavelength is changed, and a shorter wavelength can be detected by the PD.

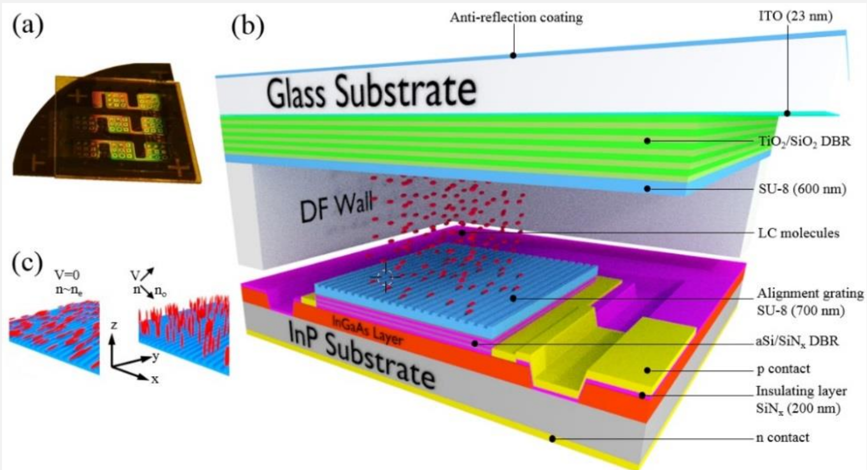

Photodetection measurements performed thanks to a tunable laser demonstrated a wavelength sweeping for the PD from 1480 nm to 1561 nm limited by the tuning range of the laser. This spectral window is covered with a LC driving voltage of 7V only, corresponding to an extremely low power consumption of few µW. The quality of the filter integrated onto the surfaces of the PD is constant over the full tuning range, showing a FWHM of 1.5 nm and a transmittance of 70%. With such features the demonstration of this Tun-PD as a micro-spectrometer has been also achieved.

More Information

- doi.org/10.1117/12.2322138

Collaborations

- Laboratoire d'Analyse et d'Architecture des Systèmes (France)
- Centre de Nanosciences et de Nanotechnologies (France)
- Institut Mines-Telecoms Atlantique (France)

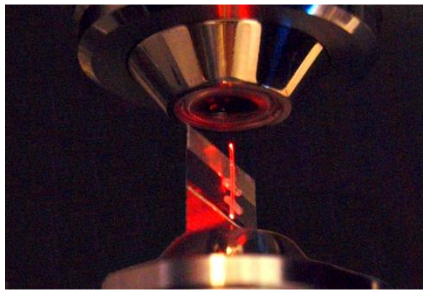

WAVEGUIDE DESIGN FOR MICRO-RING RESONATOR SENSING APPLICATIONS

SP

The development of sensors to detect various molecules including gas, proteins or viruses has an important role in societal applications such as food safety, environmental monitoring, health and defense. Such sensors must provide a fast, sensitive and selective detection response with a low limit of detection (LOD). In this context, the design of Porous Silicon (PSi) integrated micro-resonators is studied for both surface and homogeneous sensing, of grafted or solubilized analytes respectively, at 1550 nm. The aim is to optimize the sensitivity and LOD of the sensor as a function of the porosity, dimensions and propagation losses of PSi ridge waveguides for homogeneous and surface sensing (figures 1a-1b). A model for estimating the different contributions to the losses of PSi waveguides as a function of the dimensions and the porosity is then developed to allow calculation of the performances of the sensor. Low refractive index difference and high porosities mean that higher sensor performances can be obtained due to the reduction of surface scattering losses as the waveguide dimensions become larger.
The sensitivity and LOD calculated for optimized dimensions and porosities of PSi ridge waveguides are respectively 0.04 nm/(pg. mm^{-2}) and 0.5 pg.mm^{-2} for Bovin Serum Albumin (BSA) molecules surface sensing which are higher than the state of the art. For homogeneous detection (figures 1c-1d), a promising sensitivity of 800 nm/RIU (Refractive Index Unit), higher than the sensitivities that can be currently obtained with one micro-resonator, has been estimated. A LOD of 1.2.10^{-4} RIU, which is within the range of the state of the art of micro-resonator based biological sensors, has also been calculated for homogeneous detection. These promising results obtained by the optimization of the porosity and the ridge waveguide dimensions with respect to optical losses reinforce the attraction of PSi for integrated optical sensing applications.

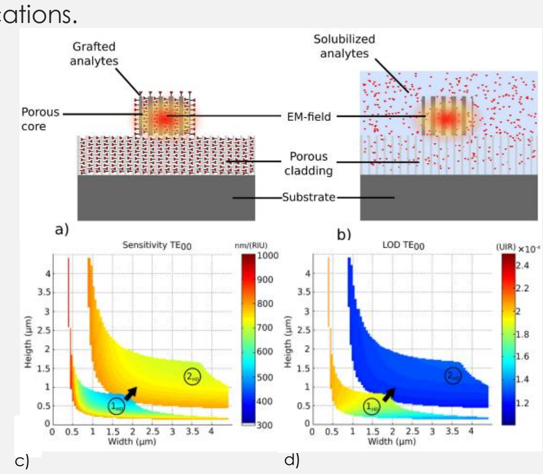

Figure 1: a) Surface and b) Homogeneous sensing applications;
c) Homogeneous sensitivity and d) LOD, as a function of the waveguide dimensions for 1_{HD} and 2_{HD} configurations:

Waveguide	Sensitivity (nm/RIU)	LOD (RIU)	Γ_{core} (%)	$\Gamma_{superstrate}$ (%)	$\Gamma_{cladding}$ (%)	Losses dB cm^{-1}	Dimensions $h \times w$ (μm^2)
$1_{HD,opt}$	700	1.2×10^{-4}	34.1	22.5	43.4	41.3	0.25×4
$2_{HD,opt}$	800	1.4×10^{-4}	32.4	5.4	62.2	37.5	0.5×4

Contact

nathalie.lorrain@univ-rennes1.fr
mohammed.guendouz@univ-rennes1.fr
monique.thual@univ-rennes1.fr

Reference

"Optimization of porous silicon waveguide design for micro-ring resonator sensing applications", P.Azuelos *et al.*, *J. Opt.* **20** 085301 (aug 2018)

hal-01891887

« Calculations now give new guidelines for PSi waveguide design in case of sensing applications »

More Information

- Pauline Girault PhD thesis (2016)
- Paul Azuelos PhD thesis (2018)
- Funded by Région Bretagne & Lannion-Trégor Communauté

Collaborations

- Institut Charles Gerhardt Montpellier (France)

Contact

olivier.durand@insa-rennes.fr

Reference

"Light-induced lattice expansion leads to high-efficiency perovskite solar cells", H. Tsai *et al.*, *Science* **360** (6384) 67-70 (apr 2018)

hal-01760080

« Light-induced lattice expansion benefits the performances of a mixed-cation pure-halide planar device, boosting the power conversion efficiency »

More Information

- doi.org/10.1126/science.aan2301
- hal.archives-ouvertes.fr/hal-01316289
- doi.org/10.1126/science.aaa5333

Collaborations

- Los Alamos National Laboratory (USA)
- Purdue University (USA)
- Northwestern University (USA)
- Argonne National Laboratory (USA)
- Rice University (USA)

HIGHLIGHTS

Light-induced high-efficiency perovskite solar cells

OHM

Recent breakthroughs in the power conversion efficiency of hybrid perovskites have been achieved by compositional engineering of the ABX_3 structure, where A and B are cations and X is an anion, in mixed-cation mixed-halide perovskites. This approach allows the formation of a stable cubic phase with suppressed nonradiative recombination for exceptionally high open-circuit voltage and short-circuit current density. However, light-induced structural dynamics plays a vital role in the physical properties, device performance, and stability of hybrid perovskite–based optoelectronic devices. We report that continuous light illumination leads to an uniform lattice expansion in hybrid perovskite thin films, which is critical for obtaining high-efficiency photovoltaic devices. Correlated, in situ structural and device characterizations reveal that light-induced lattice expansion benefits the performances of a mixed-cation pure-halide planar device, boosting the power conversion efficiency from 18.5 to 20.5 %. The lattice expansion leads to the relaxation of local lattice strain, which lowers the energetic barriers at the perovskite-contact interfaces, thus improving the open circuit voltage and fill factor. The light-induced lattice expansion did not compromise the stability of these high-efficiency photovoltaic devices under continuous operation at full-spectrum 1-sun illumination for more than 1500 hours.

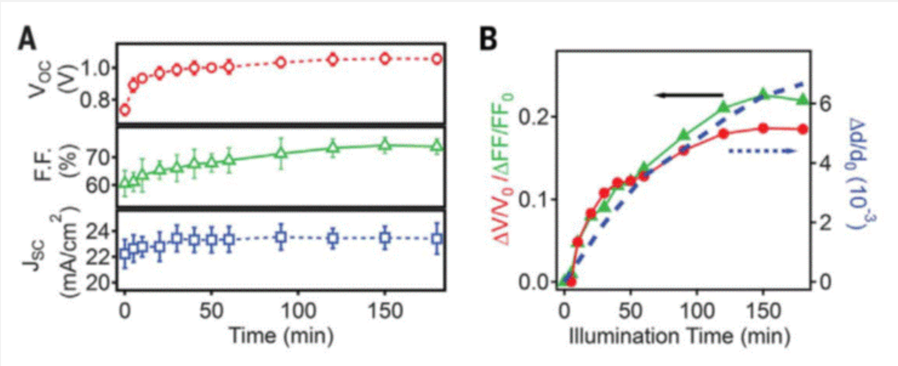

Effect of light-induced lattice expansion on PV performance of $FA_{0.7}MA_{0.25}Cs_{0.05}PbI_3$ thin films. (A) Solar cell figures of merit as a function of illumination time. Error bars indicate statistical variation over 30 devices. (B) Changes in V_{OC} and FF ($\Delta V/V_0$ and $\Delta FF/FF_0$) correlated to the change in the lattice constant ($\Delta d/d_0$) as a function of light-soaking time, where V_0 and FF_0 are the initial points before illumination

Experimental demonstration of hot carrier effect in solar cells

OHM

Contact

soline.boyer-richard@insa-rennes.fr

Reference

"Quantitative experimental assessment of hot carrier-enhanced solar cells at room temperature", D.T.Nguyen *et al.*, *Nat. Energy* **3** 236–242 (mar 2018)

hal-01745902

In common photovoltaic devices, the part of the incident energy above the absorption threshold quickly ends up as heat, which limits their maximum achievable efficiency to far below the thermodynamic limit for solar energy conversion. In a silicon solar cell, the mainstream technology, about 40% of the absorbed light energy is lost by thermalization. Conversely, the conversion of the excess kinetic energy of the photogenerated carriers into additional free energy would be sufficient to approach the thermodynamic limit. This is the principle of hot carrier devices. Unfortunately, such device operation in conditions relevant for utilization has never been evidenced.

Here, we show that the quantitative thermodynamic study of the hot carrier population, with luminance measurements, allows us to discuss the hot carrier contribution to the solar cell performance. We demonstrate that the voltage and current can be enhanced in a semiconductor heterostructure due to the presence of the hot carrier population in a single InGaAsP quantum well at room temperature.

For this purpose, we fabricated a QW-based p–i–n hot carrier solar cell prototype and investigated its optical and electrical properties. To investigate hot carrier effects, we have analysed photoluminescence (PL) and electroluminescence spectra from which one may extract thermodynamic quantities such as the temperature and the chemical potential of radiation.

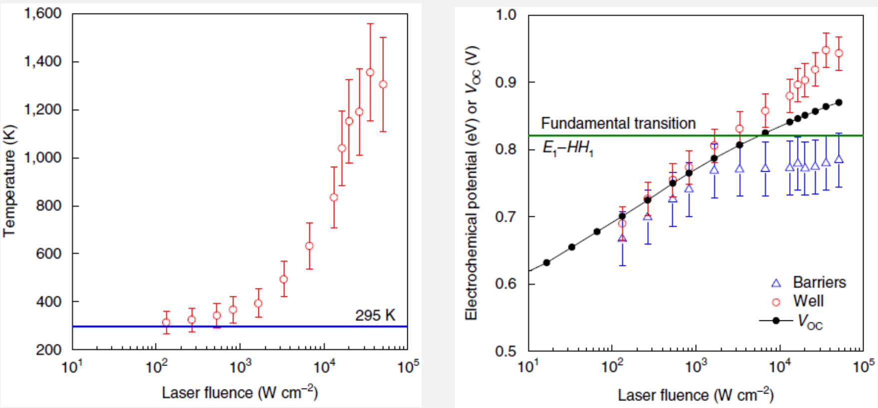

Variation of QW carrier temperature T_w and electrochemical potentials in the QW μ_w (red circles) and barriers μ_b (blue triangles) with laser power.

From luminescence spectra at different laser excitation powers, the carrier temperature T and the quasi-Fermi level splitting $\mu = E_{Fn} - E_{Fp}$ (where E_{Fn} and E_{Fp} are the electron and hole Fermi levels) are determined according to the generalized Planck law. Therefore, the fact that μ_w is higher than the fundamental transition E_1–HH_1 would indeed indicate that the barriers are allowing for isentropic cooling of the carriers, which corroborates hot carrier solar cell functionality.

« Current state-of-the-art semiconductor heterostructures can already boost solar energy conversion by hot carrier mechanisms»

Collaborations

- Institut Photovoltaïque d'Ile de France (France)

ENTROPY IN HALIDE PEROVSKITES

OHM

Halide perovskites have undeniably remarkable characteristics, which are interesting for next-generation technologies. Yet results that suggest moderate diffusion lengths and mobilities for their charge carriers are hard to reconcile with other experimental observations pointing towards long carrier lifetimes, low effective masses of carriers or short Urbach tails in the absorption spectrum. Moreover, exciton screening at room temperature, hot carrier effects and the relaxation of carriers toward the band edges are other important microscopic processes that remain poorly understood. Providing a clear picture of the behaviour of these materials has proved challenging, partly because all the above mentioned optoelectronic properties are affected by the unusually strong structural fluctuations undergone by halide perovskites.

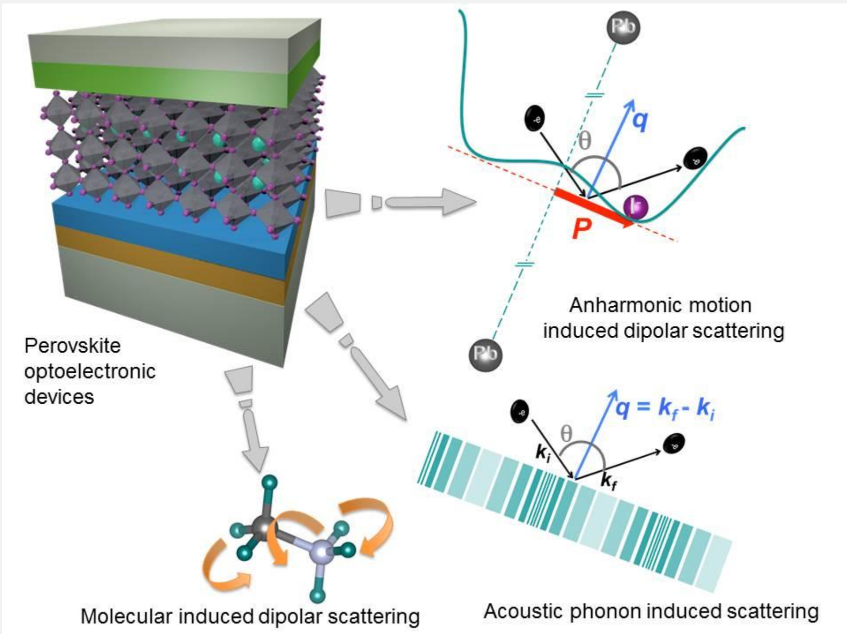

In this Nature Material volume, four teams of researchers have been invited to share their views on the current understanding of the photophysics of perovskites. They discuss some of the properties and effects that may make these semiconductors different from other materials used in optoelectronics. In this context, Claudine Katan, Aditya D. Mohite and Jacky Even discuss the possible impact of various entropy contributions (stochastic structural fluctuations, anharmonicity and lattice softness) on the optoelectronic properties of halide perovskite materials and devices.

Contact

jacky.even@insa-rennes.fr

Reference

"Entropy in halide perovskites", C.Katan *et al.*, *Nat. Mater.* **17** 377–379 (apr 2018)

hal-01774679

« Charge carriers moving in hybrid perovskite compounds find a highly perturbed electrostatic landscape, owing to stochastic structural fluctuations of the organic and inorganic components and, more broadly, to all the sources of lattice softness »

More Information

- hal.archives-ouvertes.fr/hal-01242390
- doi.org/10.1103/PhysRevB.92.201205
- doi.org/10.1021/acs.jpclett.7b00807
- hal.archives-ouvertes.fr/hal-01362483

Collaborations

- Institut des Sciences Chimiques de Rennes (France)
- Rice University (USA)
- Los Alamos National Laboratory (USA)

BUFFER RESERVOIR NOISE CANCELLATION IN DUAL FREQUENCY LASER

DOP

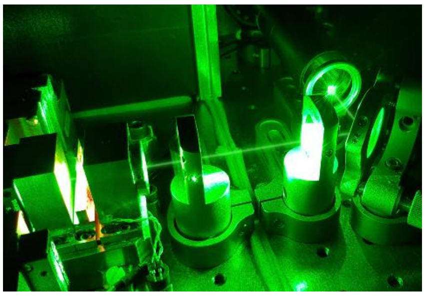

Low amplitude noise lasers are sought after for a large variety of applications among which metrology, microwave photonics, Lidar-Radar, optical clocks, low noise sensing, atom manipulation and coherent communications. We have been developing over the past year a novel approach aiming at breaking the resonant exchanges between photon and gain populations inside the laser cavity. This so-called "Buffer Reservoir" (BR) approach relies on the insertion of optimized low efficiency and fast nonlinear absorption within the laser cavity leading to noise reduction up to 50 dB. The BR principle has been validated in single frequency solid-state lasers using two-photon absorption as well as second harmonic depletion. 50 dB noise reduction was achieved, i.e. a hundred times better than any electronic loop, without degrading neither the laser power nor its phase noise. Moreover, the potential of this technic in terms of noise reduction has been demonstrated at frequencies never reached before by any noise reduction approach, i.e., several tens of GHz, enabling the cancelation of the excess noise appearing at the harmonics of the free spectral range of the laser. The thorough modelling of the underlying physics led us to extend the Buffer reservoir principle to dual frequency lasers where additional excess noise contributions appear at the in-phase and anti-phase relaxation oscillations. More than 40 dB reduction has been obtained in dual frequency solid state lasers at both in-phase and anti-phase relaxation oscillation frequencies which was never achieved yet by any other method. By overcoming the previous generation of low noise Class A lasers this work paves the way to several new opportunities in numerous applied and fundamental research domains including quantum photonics.

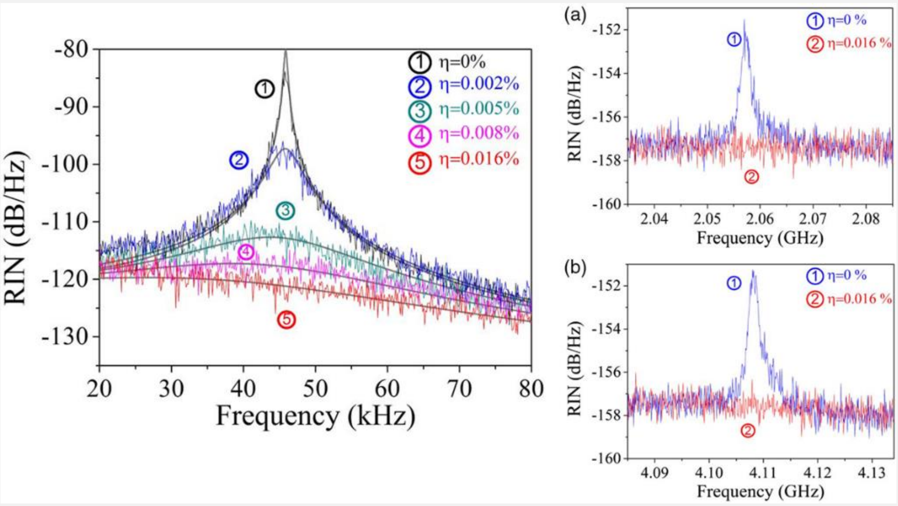

This research was conducted in the framework of the ASTRID project MINOTOR and the European Defense Agency project HIPOMOS. K. Audo's PhD Thesis was funded by the French Defence Agency (DGA), Région Bretagne and Thales. The post-doctoral fellow of A. El Amili supported by CNRS

Contact

mehdi.alouini@univ-rennes.fr

Reference

"Analytical modeling of dual-frequency solid-state lasers including a buffer reservoir for noise cancellation", K.Audo *et al.*, *Opt. Express* **26** 8805-8820 (apr 2018)

hal-01786645

« Buffer Reservoir lasers: the new generation of low intensity noise coherent sources »

More Information

- hal.archives-ouvertes.fr/hal-01786640
- doi.org/10.1109/MWP.2016.7791273
- doi.org/10.1364/OL.41.004237
- doi.org/10.1364/OL.41.002326
- doi.org/10.1364/OL.40.001149
- doi.org/10.1364/OL.39.005014
- doi.org/10.1364/OE.21.008773

Collaborations

- University of California San Diego (USA)

UC San Diego
JACOBS SCHOOL OF ENGINEERING
Electrical and Computer Engineering

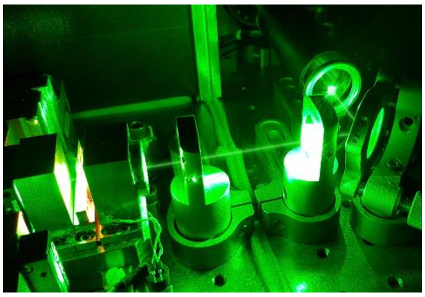

Contact

mehdi.alouini@univ-rennes1.fr

Reference

"VSPIN: a new model relying on the vectorial description of the laser field for predicting the polarization dynamics of spin-injected V(e)CSELs", M.Alouini *et al.*, *Opt. Express* **26** 6739-6757 (mar 2018)

hal-01996541

« VSPIN, the proper modelling framework for spin-lasers »

More Information

- doi.org/10.1364/OE.26.006739
- doi.org/10.1364/OE.23.009573
- doi.org/10.1063/1.4850676
- tel.archives-ouvertes.fr/tel-01127040
- Alexandre Joly PhD thesis (2018)

Collaborations

- Thales Research and Technology (France)
- Unité Mixte de Physique CNRS/Thales (France)

VSPIN THEORETICAL FRAMEWORK FOR SPIN-CONTROLLED VCSELs

DOP

Spin-lasers are attracting a lot of attention as they are expected to be the solution for conveying the electronic spin information well beyond the spin relaxation mean path (in the order of a few nm). By converting the electronic spin information into optical polarization information (right or left circular), Spin-lasers may offer a reliable solution for interconnecting future quantum computers for instance. Optimization of spin-lasers relies on a proper design of the spin injector in the active medium. Nevertheless, unlike in spin-LEDs, it has been noticed over the past years that the polarization control of spin lasers is a very difficult task. They indeed reveal spin injection effects in their transient behavior, but not in their steady state where they tend to emit linear polarizations. We have shown that the interplay between gain asymmetry and additional polarimetric effects, either within the active medium or in the resonator, rules the laser output polarization. Thus a thorough understanding of the laser polarization behavior implies a vectorial description of the transverse electromagnetic field.

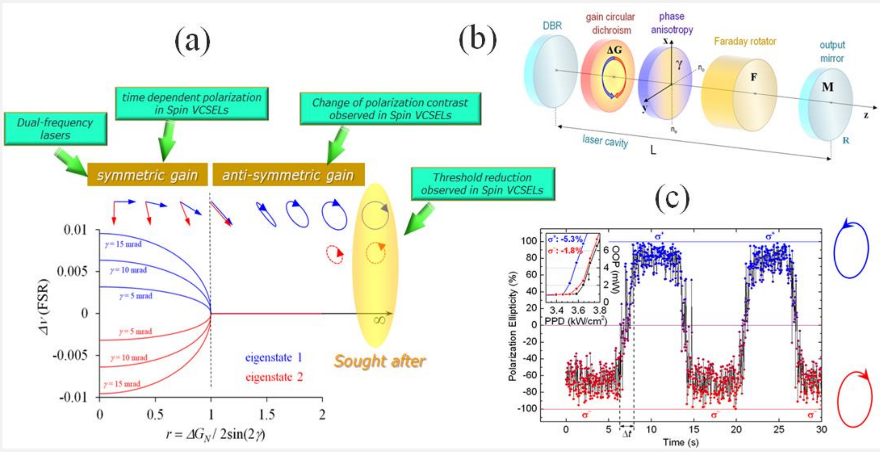

The VSPIN (Vectorial SPIN) modelling framework that we have proposed reveals the existence of two possible eigenstates which can beat together, lock together or even compete together according to the gain asymmetry strength. This leads to various time dependent or steady state polarization behaviors observed by other groups and ours. This modeling framework enabled us to overcome the detrimental effects that cause the linear polarization emission. Accordingly, a polarization ellipticity of ±30° of the output beam has been achieved in a VeCSEL in the steady state regime, at room temperature and without external magnetic field, although in these stringent conditions only a fraction of percent of gain asymmetry is induced due to the fast electronic spin relaxation. Besides, the VSPIN formalism guided us to imagine a laser whose two eigen-polarizations are inherently right- and left-handed circular. Owing to mode coupling between the two possible eigenstates, full polarization switching has been predicted and observed despite the very weak spin injection efficiency. Such a leverage effect, which is not present in spin-LEDs, is an additional interesting feature towards the realization of efficient and compact spin-lasers.

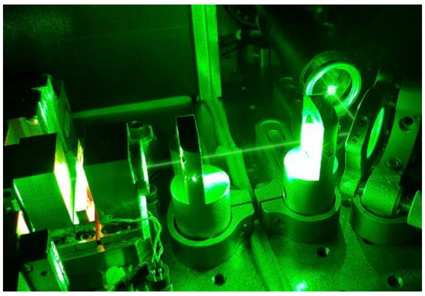

BLUE LASER DIODE INTENSITY FLUCTUATIONS

SP

Since the first commercially available GaN based laser diodes in 1999, blue emitting coherent sources have opened up new opportunities in areas such as optical data storage, visible light communication, linear and nonlinear spectroscopy for fundamental and industrial applications, pico-projection and lighting. Without being exhaustive, this list highlights the benefits offered by GaN lasers. In the aforementioned applications, the stability of the laser intensity is one of the key parameters. Indeed, for applications that use modulation in the MHz to GHz range, like data storage, VLC and pico-projection, the intensity noise has to be calibrated on the targeted bandwidth. In the same vein, for spectroscopic applications for which the signal to noise ratio is the relevant parameter, the noise of the laser is the limiting parameter and has to be quantified. A deep understanding of the dynamics of InGaN lasers is mandatory since it affects the overall characteristics of the devices in which they might be embedded.

In lasers, the noise response is directly governed by the photon and the electron populations dynamics. In particular, in monolithic semiconductor lasers, the two populations dynamics are coupled and energy exchange occurs at a frequency called the relaxation frequency. Intensity noise is one of the observable allowing a better understanding of the impact of the structure on the laser dynamics. Indeed, both the cavity design (photon population) and the epitaxial structure (electron population) directly impact on the noise dynamics. Commercially available blue laser diodes are edge-emitting Fabry-Perot-type cavity laser that usually exhibits multimode emission causing instabilities in the output beam.

Despite their importance, the correlations existing, in blue emitting laser diodes, between the optical spectrum structure and intensity fluctuations mediated by noise have not been addressed surprisingly.

The laser diodes under test are designed, grown and processed by our colleagues from the Laboratory of Advanced Semiconductors for Photonics and Electronics at Ecole Polytechnique Fédérale de Lausanne (EPFL) in Switzerland. To reveal the impact of the modal structure on the intensity dynamics of InGaN edge emitting laser diodes, we record simultaneously the relative intensity noise (RIN) and the optical spectrum of the output laser beam. We show that for specific pump current operations, the laser may display a variety of lasing regimes, each of them featuring their own intensity noise signature. This study reports that InGaN edge emitting laser diodes can manifest strong intensity dynamics that can even be detrimental for specific purposes. An analytical model, reproducing our experimental observations, suggests that gain compression coupled to asymmetric mode amplification are at the origin of the intensity instability of the laser. The multimode nature of those lasers strongly favors intensity fluctuations. An attractive solution would be the design of stable single mode lasers. Currently, only external cavity architecture can offer single mode laser diode operation in the blue wavelength range hence highlighting the need to develop monolithic single mode InGaN laser diodes.

Contact

stephane.trebaol@enssat.fr

Reference

"Impact of Mode-Hopping Noise on InGaN Edge Emitting Laser Relative Intensity Noise Properties", A. Congar *et al.*, *IEEE J. Quantum Electron.* **54**(1) 1100107 (feb 2018)

hal-01959531

« Why blue laser diodes exhibit strong intensity noise? »

More Information

- doi.org/10.1143/APEX.3.092102

Collaborations

- Ecole Polytechnique Fédérale de Lausanne (Switzerland)

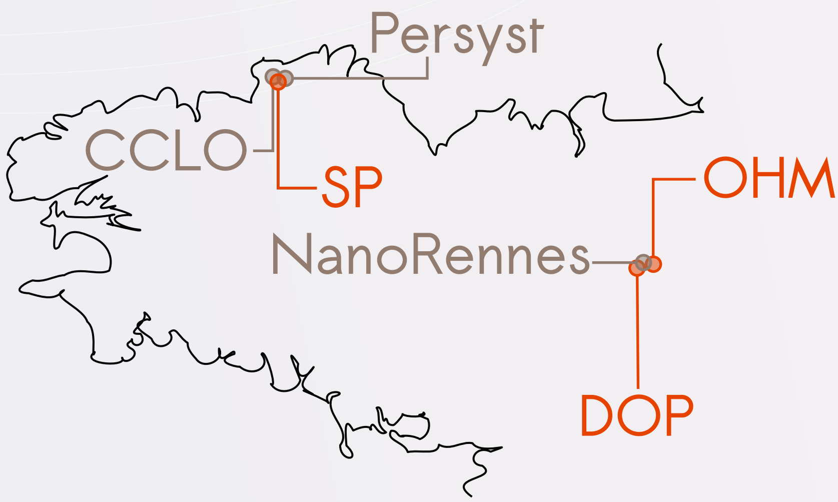

3 teams + 3 platforms

A leading-edge research in photonics

Devices and functionalities for optical communications

Microwave, Millimeter and Tera-Hertz Optics

Innovative materials for Photonics

Instrumentation, Optical Sensors and Coherent Imaging

Advanced concepts for Photovoltaics

Lasers Physics and Metrology

Technological transfer support, strong industrial partnerships, international collaborations

Trainings in photonics: engineering schools, master's degree, DUT...

http://foton.cnrs.fr